

Article

3'-Aminothiocylohexanespiro-5'-hydantoin and Its Pt(II) Complex—Synthesis, Cytotoxicity and Xanthine Oxidase Inhibitory Activity

Emiliya Cherneva ^{1,2}, Mariyana Atanasova ¹, Žaklina Šmelcerović ³, Katarina Tomović ⁴, Rossen Buyukliev ¹, Andrija Šmelcerović ^{5,*} and Adriana Bakalova ^{1,*}¹ Department of Chemistry, Faculty of Pharmacy, Medical University of Sofia, 2 Dunav Str., 1000 Sofia, Bulgaria² Institute of Organic Chemistry with Centre of Phytochemistry, Bulgarian Academy of Sciences, Acad. G. Bonchev Str., Build 9, 1113 Sofia, Bulgaria³ Center for Biomedical Science, Faculty of Medicine, University of Niš, Bulevar Dr Zorana Đinđića 81, 18000 Niš, Serbia⁴ Department of Pharmacy, Faculty of Medicine, University of Niš, Bulevar Dr Zorana Đinđića 81, 18000 Niš, Serbia⁵ Department of Chemistry, Faculty of Medicine, University of Niš, Bulevar Dr Zorana Đinđića 81, 18000 Niš, Serbia

* Correspondence: andrija.smelcerovic@medfak.ni.ac.rs (A.Š.); adrigebk@abv.bg or a_bakalova@pharmfac.mu-sofia.bg (A.B.)



Citation: Cherneva, E.; Atanasova, M.; Šmelcerović, Ž.; Tomović, K.; Buyukliev, R.; Šmelcerović, A.; Bakalova, A. 3'-Aminothiocylohexanespiro-5'-hydantoin and Its Pt(II) Complex—Synthesis, Cytotoxicity and Xanthine Oxidase Inhibitory Activity. *Inorganics* **2022**, *10*, 175. <https://doi.org/10.3390/inorganics10100175>

Academic Editors: Hristo P. Varbanov and Vladimir Arion

Received: 8 August 2022

Accepted: 18 October 2022

Published: 20 October 2022

Publisher's Note: MDPI stays neutral with regard to jurisdictional claims in published maps and institutional affiliations.



Copyright: © 2022 by the authors. Licensee MDPI, Basel, Switzerland. This article is an open access article distributed under the terms and conditions of the Creative Commons Attribution (CC BY) license (<https://creativecommons.org/licenses/by/4.0/>).

Abstract: Herein, we report the synthesis of platinum(II) complex bearing 3'-aminothiocylohexanespiro-5'-hydantoin as ligand. The complex was characterized by IR, NMR spectral analyses, elemental analyses and density functional theory (DFT) calculations. Cytotoxicity and inhibitory potential on xanthine oxidase (XO) were evaluated by performed docking calculations. The cytotoxic activities of the 3'-aminothiocylohexanespiro-5'-hydantoin (**1**), its Pt(II) complex (**2**), thiocylohexanespiro-5'-hydantoin (**3**), and its platinum complex (**4**) were assessed against HL-60 and MDA-MB-231 cells in comparison with the antiproliferative activity of cisplatin as a referent. The ligands (**1** and **3**) did not exhibit *in vitro* antitumor efficacy on either of the human tumor cell lines. Complex **2** showed higher antitumor activity (IC₅₀ = 42.1 ± 2.8 μM on HL-60 and 97.8 ± 7.5 μM against MDA-MB-231 cells) than complex **4** (IC₅₀ = 89.6 ± 2.8 μM on HL-60 and 112.5 ± 4.2 μM in MDA-MB-231 cells). IC₅₀ values of cisplatin as referent were 8.7 ± 2.4 μM on HL-60 and 31.6 ± 5.4 μM on MDA-MB-231 cell lines. The inhibitory activity of ligands and complexes against XO, evaluated *in vitro*, were compared with allopurinol (IC₅₀ = 1.70 ± 0.51 μM) as standard inhibitor. The platinum(II) complexes (**2** and **4**) inhibited the activity of XO, with IC₅₀ values 110.33 ± 26.38 μM and 115.45 ± 42.43 μM, respectively, while the ligands **1** and **3** did not show higher degrees of inhibition at concentrations lower than 150 μM. The inhibitory potential against XO might be a possible precedent resulting in improved profile and anticancer properties.

Keywords: platinum complexes; hydantoin; cytotoxicity; xanthine oxidase inhibition

1. Introduction

Metal complexes are considered to be an extremely important class of compounds in medicine and medicinal chemistry because of their diverse pharmacological applications. Many complexes act as antioxidant, antibacterial, antiviral, analgesic, antimicrobial and anticancer agents [1–3]. Transition metal complexes have been extensively investigated as chemotherapeutic agents. Platinum-based anticancer agents have become the most common class used in chemotherapy worldwide [4,5]. Anticancer drugs that have been used in cancer therapy have serious well-known side effects [6–8]. To increase bioavailability, enhance cytotoxicity, and reduce side effects in comparison to cisplatin, a new class of Pt(II) complexes [9,10] was synthesized.

Hydantoins (imidazolidinediones) are small molecules that possess different biological and pharmaceutical applications, including as anticonvulsants, antiarrhythmics, antibacterial and antitumor agents [11–13]. A series of spirohydantoins were studied and evaluated as promising anticancer compounds in our earlier research [14,15].

The tumor growth causes tissue damage that provokes the inflammatory response and possible increase in the activity and the expression of xanthine oxidase (XO) in plasma. The activation of carcinogenic compounds can be catalyzed by this oxidase. Xanthine oxidase might also act tumorigenically by producing reactive oxygen and nitrogen species [16]. Despite being rare [17], there are data on metal complex-based inorganic XO inhibitors [18–23].

The present paper describes the synthesis, characterization, cytotoxic activity and inhibitory potential on XO of a new platinum complex (complex 2). The biological activities of 3'-aminothiocyclohexanespiro-5'-hydantoin (1) and thiocyclohexanespiro-5'-hydantoin (3) were compared with those of their platinum complexes (2 and 4) (Figure 1). To define the docking interactions of Pt complex–XO complex, docking calculations were performed.

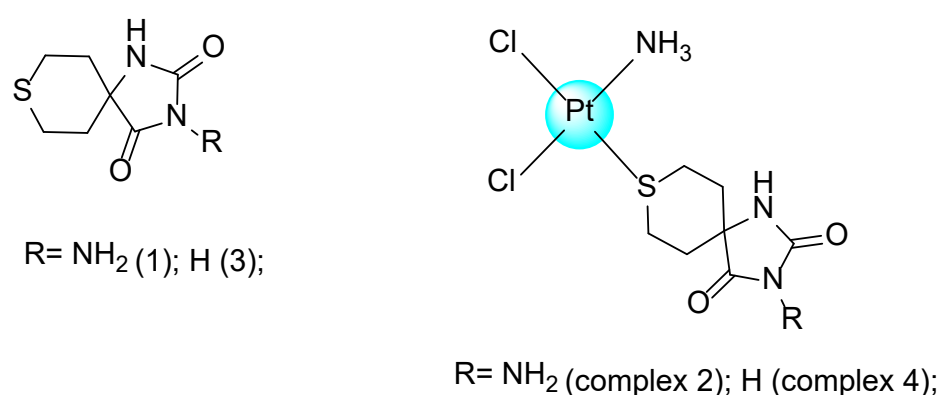


Figure 1. Structural formulas of ligands 1 and 3 and complexes 2 and 4.

2. Results and Discussion

2.1. Synthesis

On the basis of our previous investigations [24], the structure of thiocyclohexanespiro-5'-hydantoin was essential for the platinum complexes to possess the potent XO inhibitory activity. Therefore, we synthesized a new Pt(II) complex with 3'-aminothiocyclohexanespiro-5'-hydantoin as ligand. The complex was synthesized *via* one-step reaction by mixing K[Pt(NH₃)Cl₃] with the ligand in a stoichiometric ratio of 1:1 under mild conditions and good chemical yield.

2.2. Spectral Characterization and Geometry Optimization

2.2.1. Spectral Analysis

The coordination of the ligand with platinum ion was demonstrated by comparing of the IR spectra of the ligand 1 and complex 2. The stretching vibrations corresponding to the C–S bond are observed at 655 cm^{−1} in ligand 1, while in complex 2, $\nu(\text{C–S})$ is at 625 cm^{−1}. This decrease of 30 cm^{−1} is due to the fact that the ligand bonds with the metal ion via the sulphur atom from the thiocyclohexane moiety. The NH and $\nu(\text{C=O})$ stretching are slightly affected upon coordination. The IR spectra of the new complex 2 and the ligand 1 in the far IR below 400 cm^{−1} region were also recorded, where metal–halogen stretching vibrations occur. Two absorption bands at 330 and 319 cm^{−1} are assignable to Pt–Cl stretching. The doublet character of these bands is an indication of the *cis*-configuration of the complex [25–27]. Moreover, the method for obtaining of the new complex supposed the synthesis of a *cis*-isomer according to the literature [28]. For example, for the synthesis of the *cis*-isomer, K[Pt(NH₃)Cl₃] as a starting complex is used, while for the synthesis of the *trans*-isomer, the other starting complex—*cis*-[Pt(NH₃)₂Cl(NO₃)]—is used. Starting from K[PtCl₃NH₃], the reaction with ligand 1 leads to substitution of one of the two *trans*-

chlorides (both *cis* to the ammine), which are mutually *trans*-labilized [29] (Supplementary Materials Figures S1 and S2).

A comparison of the ^1H NMR spectra of pure ligand **1** and complex **2** indicates a chemical shift difference of 0.20 ppm for the axial protons from CH_2 groups connected to the sulphur atom. This chemical change is proof of the coordinative bonding between the sulphur atom and platinum ion (Supplementary Materials Figures S3 and S4).

There is no great difference between the chemical shifts of the carbon atoms in the ^{13}C NMR spectra of the metal-free ligand **1** and complex **2** (Supplementary Materials Figures S5 and S6).

2.2.2. Quantum Chemical Modeling

Being unable to grow single crystals, quantum chemical studies were applied to explore the structure and the way of bonding of the Pt ion with the ligand using the B3LYP/6-31+G(d) level for nonmetals and LANL2DZ for platinum. In Figure 2, the optimized structures of the studied compounds are presented. In our previously published work [30], the optimized molecular geometry of ligand **1** was described in detail. To investigate the geometrical structure of the complex, two possible *cis*-conformations are optimized, namely boat and chair, by taking into account the position of spiro C-atom around platinum center. The calculations in the gaseous state show that the boat conformation is energetically more favorable by 16 kJ/mol than chair. This result is similar to that found in our previous calculations on the thiocyclohexanespiro-5'-hydantoin complex [30].

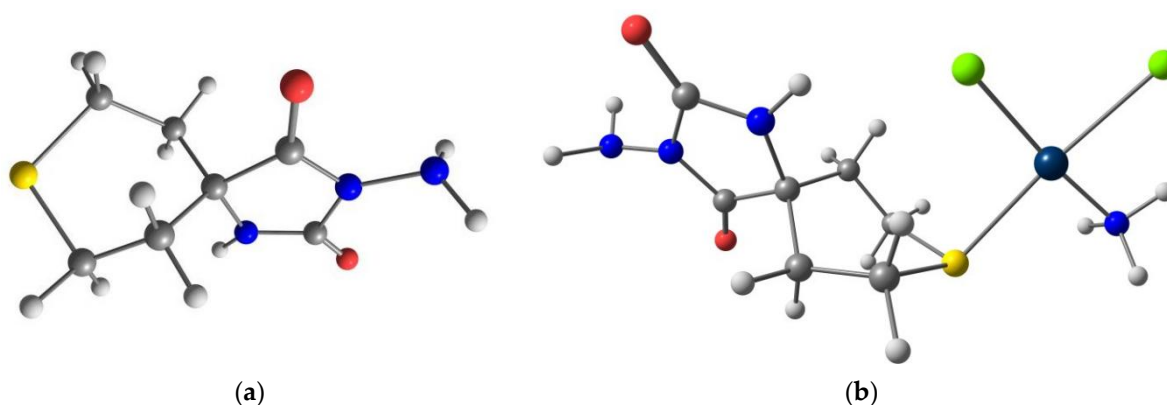


Figure 2. Optimized structures of ligand **1** (a) and complex **2** (b).

Pt(II) ion is located in the center of a slightly distorted square planar coordination geometry. The Pt-Cl (2.41 Å), Pt-S (2.45 Å) and Pt- $\text{N}_{\text{ammonia}}$ (2.09 Å) bond lengths are similar or close to values observed for other optimized square planar complexes [31–35]. After coordination of the ligand with the platinum ion, the ligand geometry will not change significantly, according to the theoretical analysis. The lengthening of the C-S bonds by 0.07–0.08 Å is probably due to the bonding of the ligand with the Pt ion.

To prove the *cis*-configuration of complex **2**, IR spectra of *cis*- and *trans*-isomers were calculated. In comparing these two spectra, small differences can be observed. However, when comparing of the calculated IR spectra for *cis*- and *trans*-isomers with the experimental data, it can be observed that the experimental IR spectrum is close to the theoretical spectrum of the *cis*-isomer. The fact that the theoretical spectrum was made in the gas phase, while the experimental spectrum was made in the solid phase, should be taken into account (Supplementary Materials Figure S7)

2.3. Biological Evaluation

2.3.1. Antiproliferative Activity

In vitro cytotoxicity of the new complex **2** proved to be significant within this series of compounds. Complex **2** showed higher antitumor efficacy against HL-60 and MDA-MB-231 than complex **4** and the ligands (**1** and **3**). IC₅₀ values were $42.1 \pm 2.8 \mu\text{M}$ for complex **2** and $89.6 \pm 2.8 \mu\text{M}$ for complex **4** on the HL-60 cell line and $97.8 \pm 7.5 \mu\text{M}$ for complex **2**, and $112.5 \pm 4.2 \mu\text{M}$ for complex **4** on the MDA-MB-231 cell line. Ligands **1** and **3** did not exhibit *in vitro* antiproliferative activity on either of the human tumor cell lines. IC₅₀ values of cisplatin as a referent were $8.7 \pm 2.4 \mu\text{M}$ on HL-60 and $31.6 \pm 5.4 \mu\text{M}$ against MDA-MB-231 cell lines.

2.3.2. XO Activity

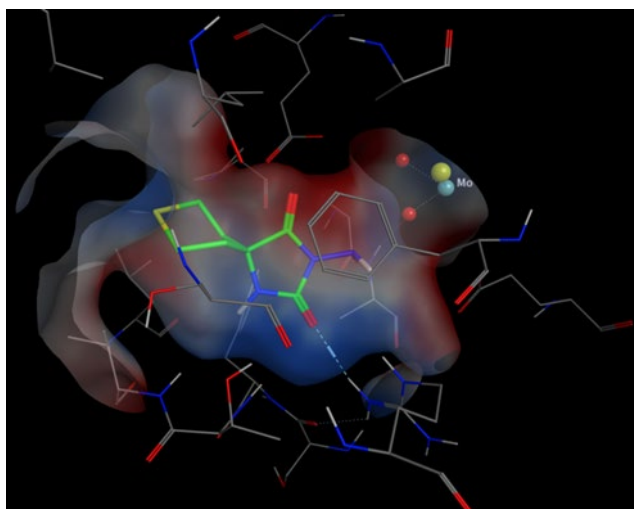
The platinum(II) complexes (**2** and **4**) inhibited the activity of XO, with IC₅₀ values $110.33 \pm 26.38 \mu\text{M}$ and $115.45 \pm 42.43 \mu\text{M}$, respectively, while ligands **1** and **3** did not show a higher degree of inhibition at concentrations lower than $150 \mu\text{M}$. The IC₅₀ value of allopurinol as a standard inhibitor was $1.70 \pm 0.51 \mu\text{M}$.

3. Molecular Docking Study

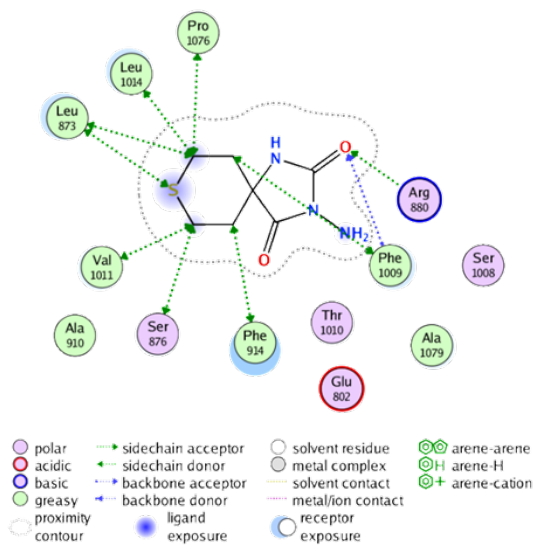
The best docking scores with the lowest Affinity dG value of ligands **1** and **3** and Pt(II) complexes **2** and **4** are given in Table 1. The corresponding binding poses at the XO binding site are depicted in Figure 3. Ligand **1** forms a hydrogen bond between the O atom of CO group at the fourth position and the hydrogen atom of the guanidino group of Arg880 (Figure 3A,B). Additionally, Van der Waals interactions stabilize the predicted pose. In the case of ligand **3** molecule, only weak Van der Waals interactions occur (Figure 3E,F). Both molecules are characterized by the low Affinity dG score of the docking calculations (Table 1). This is possibly due to the fact that both ligands **1** and **3** are placed close to the entrance, rather than deep in the binding pocket, where the molybdenum center is located.

Table 1. The lowest Affinity dG scores of the studied compounds docked in bovine xanthine oxidase enzyme.

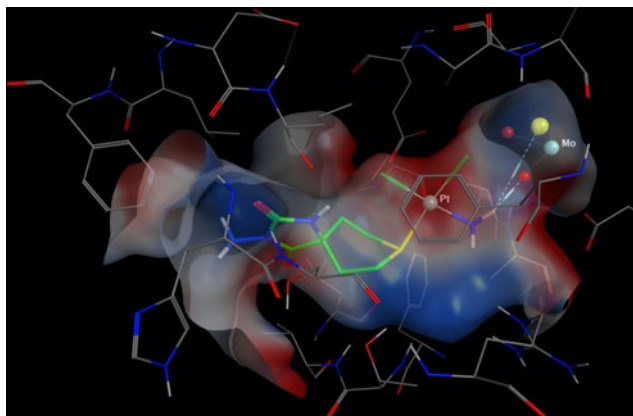
Compound	Affinity dG
Ligand 1	−3.9795
Complex 2	−6.5197
Ligand 3	−3.4150
Complex 4	−6.7772



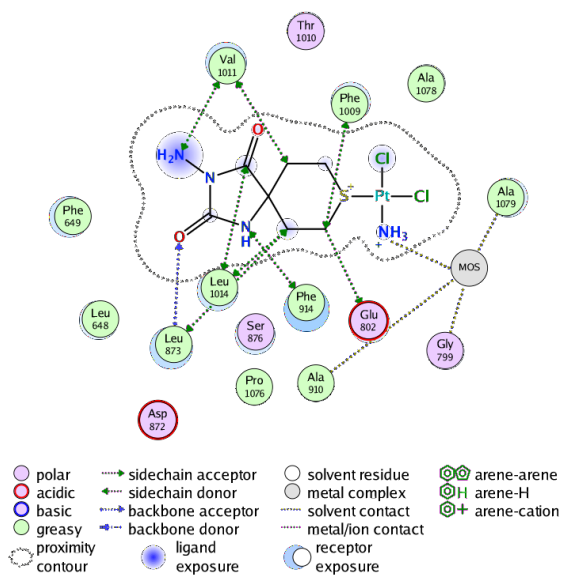
(A)



(B)



(C)



(D)

Figure 3. Cont.

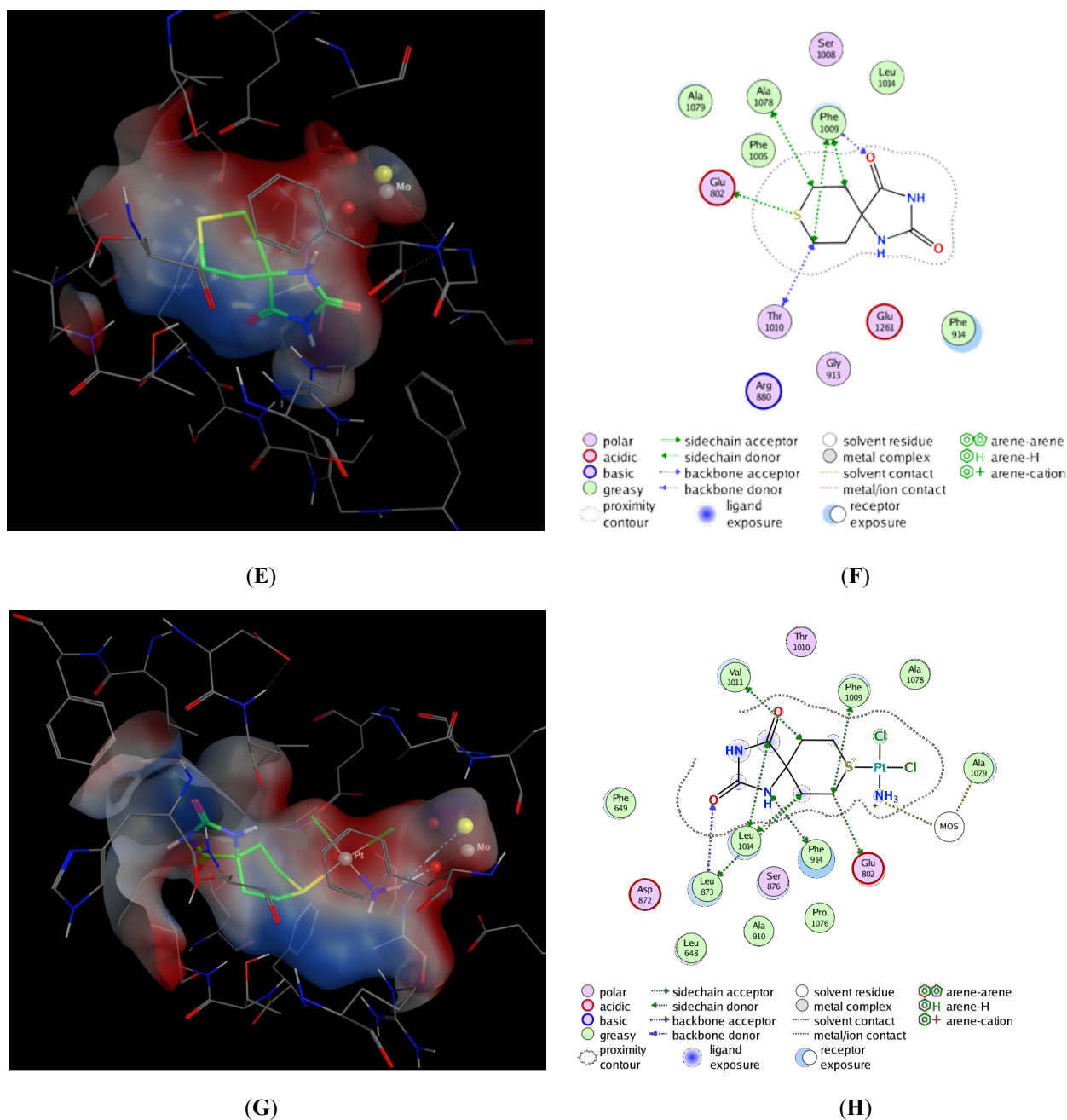


Figure 3. Docking poses and interaction diagrams of ligand (1) (A,B), (complex 2) (C,D), ligand (3) (E,F) and (complex 4) (G,H). Visualization of coordinative bonds in the MOE package is denoted as positively charged atoms.

The best predicted poses of complexes 2 and 4 insert deep into the pocket, close to the molybdenum atom (Figure 3C,D,G,H). The coordinative bond of ammonium group links with oxygen and sulfur atoms of MOS. In addition, Van der Waals interactions stabilize the complexes. This results in higher Affinity dG values in both molecules (Table 1).

4. Materials and Methods

Thiocyclohexanespiro-5'-hydantoin is available by means of Bucherer–Berg reaction from $(\text{NH}_4)_2\text{CO}_3$, NaCN and tetrahydro-4*H*-thiopyran-4-one (Aldrich). Potassium aminethrechloroplatinate(II) was purchased from Sigma Aldrich USA. All other chemicals used were of analytical reagent grade. The carbon, nitrogen and hydrogen content of the new compound were determined by elemental analyses on a EuroEA 3000—Single, “Euro

Vector SpA". IR spectra were recorded in the range of 4000–100 cm^{-1} on Bruker Invenio R spectrophotometer, ATR (attenuated total reflectance) mode with a diamond crystal accessory. The spectra were referenced to air as a background by accumulating 100 scans, at a resolution of 2 cm^{-1} . The ^1H NMR and ^{13}C spectra were recorded on Bruker WM 500 (500 MHz) spectrometer in dimethyl sulfoxide as a solvent. Chemical shifts are expressed to tetramethylsilane and are represented in δ (ppm). Splitting patterns were indicated by the symbols s (singlet), m (multiplet) and bs (broad singlet). The solution of complex 2 was freshly prepared in DMSO- d_6 . Melting point was determined as the phase transition from solid to liquid at atmospheric pressure, on a Buchi 540 apparatus.

4.1. Synthesis

Cis-Amminedichlorido-(3'-aminothiocylohexanespiro-5'-hydantoin) Platinum (II)—*Cis*-[PtL(NH₃)Cl₂], Complex 2

To aqueous solution of K[Pt(NH₃)Cl₃] (0.1605 g, 0.0449 mmol) was added an aqueous ethanol solution of ligand ($\phi r = 1:1$) (0.1079 g, 0.437 mmol). The reaction mixture was stirred for 10 h at ambient temperature and the solution cooled to 4 °C. The lemon-yellow precipitate was filtered off and dried in a vacuum. The purity was checked by elemental analyses. Thin-layer chromatography (TLC) is used for identifying the compound. The eluent is CH₃COOC₂H₅/C₂H₅OH— $\phi r = 2:1$. Yield: ca. 73%, m. p.: 276–277 °C (dec.). Anal. Calc. for C₇H₁₄N₄O₂SCl₂Pt: C, 17.36; N, 11.57; H, 2.89. Found: C, 17.88; N, 10.91; H, 3.31. IR (ATR, cm^{-1}): 3501, 3265, 3187, 1773, 1705, 625, 330, 319. ^1H -NMR (500MHz, DMSO- d_6 , δ , ppm): 8.64 (s, 1H, NH); 4.66 (bs, 2H, NH₂); 4.27–4.24 (m, 3H, NH₃); 2.82–2.79 (m, 2H, CH₂-S(ax)); 2.62–2.61 (m, 2H, CH₂-S(eq)); 1.92–1.87 (m, 2H, CH₂-C(ax)); 1.74–1.71 (m, 2H, CH₂-C(eq)).

4.2. Quantum Chemical Modeling

The Gaussian 03 software package was used for theoretical calculations [36]. The geometry of the ligand and its complex was performed using a gradient analytical technique. The results were obtained by B3LYP (Becke's three-parameter non-local exchange) [37,38] functional correlation, 6-311++G(g,p) basis set for all non-metal atoms, and LANL2DZ basis set for the platinum center. The optimized structures were also characterized by analytical calculations of harmonic vibrational frequencies at the same level of theory.

4.3. Biological Evaluation

A preliminary evaluation of the cytotoxic activity of complex 2, as well as of complex 4, ligands 1 and 3 and cisplatin as a referent drug, was performed on two human tumor cell lines: HL-60 and MDA-MB-231.

HL-60 is a promyelocytic leukemia cell line, while the MDA-MB-231 is a triple negative breast cancer cell line. The solid tumor cell line (MDA-MB-231) was grown as monolayer-adherent cultures in 90% RPMI-1640 medium (Cat. No. F7524, Sigma[®] Life Science, Steinheim, Germany) supplemented with 10% fetal bovine serum (FBS, Cat. No. F7524, Sigma[®] Life Science, Steinheim, Germany), non-essential amino acids, 1 mM sodium pyruvate and 10 mg/mL human insulin. The other cell line (HL-60) was grown as a suspension-type culture under standard conditions—RPMI-1640 liquid medium supplemented with 10% FBS and 2 mM L-glutamine, in cell culture flasks, housed at 37 °C in an incubator "BB 16-Function Line" Heraeus with humidified atmosphere and 5% CO₂. The cells were kept in log phase by supplementation with a fresh medium after removal of cell suspension aliquots, two or three times a week.

The cell lines were obtained from DSMZ German Collection of Microorganisms and Cell Cultures and were validated in the Laboratory of Pharmacology and Toxicology (in the Faculty of Pharmacy, Medical University of Sofia, Bulgaria) as being suitable to test metal complexes. Their DSMZ catalog numbers are HL-60 (ACC 3) and MDA-MB-231 (ACC 73). The cytotoxic effects of ligands 1 and 3 and complex 4 of the same human tumor cell lines were described in our previous study [30,33]. The cytotoxicity of the new

complex **2** was assessed using the MTT assay, as described by Mossman [39] with some modifications [40]. The method is based on the reduction of the yellow tetrazolium salt MTT [3-(4,5-dimethylthiazol-2-yl)-2,5-diphenyltetrazolium bromide] (Cat. No. M5655-1G, Sigma[®] Life Science, Steinheim, Germany) to a violet formazan via the mitochondrial succinate dehydrogenase in viable cells.

For the treatment procedures, the tested compound was freshly dissolved in DMSO, and thereafter diluted with RPMI-1640 growth medium. Our experience with water insoluble metal complexes has showed that there is no significant modulation of chemosensitivity of the individual cell lines. For each concentration, 8 separate wells were used. Every assay was carried out in three separate microplates. The MTT-formazan absorption was determined using a microprocessor-controlled microplate reader (Labexim LMR-1) at 580 nm.

4.4. Evaluation of XO Inhibition

The inhibitory properties of ligands **1** and **3** and their platinum complexes **2** and **4** on XO were evaluated *in vitro* on the commercial bovine milk enzyme by spectrophotometric measurement of uric acid formation at 293 nm, with allopurinol as a reference inhibitor, as described in our previous study [41].

4.5. Molecular Docking to Xanthine Oxidase

The ab initio optimized geometries of ligands **1** and **3** and Pt(II) complexes **2** and **4** were subject to docking calculations to the crystallographic structure of xanthine oxidase from bovine milk (pdb id: 3NRZ, R = 1.8 Å) [42]. The docking was performed using MOE2016.0801 [43] with the following settings: Placement method: triangle Matcher and scoring function AlphaHB; Refinement: induced fit with free movement of side chains and scoring function Affinity dG. In the placement step, 1000 poses of each ligand were generated using the Triangle Matcher method and 100 of them with best Alpha HB score proceeded to the next step of refinement. The five best Affinity dG-scored complexes for each ligand were kept.

5. Conclusions

The synthesis and characterization of platinum(II) complex bearing 3'-aminothiocyclohexanespiro-5'-hydantoin as ligand was reported. The experimental and theoretical data suggest coordination of Pt ion via S-donor ligand. The studied complex was documented to have promising cytotoxicity with an inhibitory activity against XO that might be an additional mechanism in the anticancer activity.

Supplementary Materials: The following supporting information can be downloaded at: <https://www.mdpi.com/article/10.3390/inorganics10100175/s1>, Figure S1: Experimental IR spectra of the ligand **1** (black) and complex **2**(red) in the range 4000–100 cm⁻¹; Figure S2: Experimental IR spectra of the ligand **1** (black) and complex **2** (red) in the range 1800–100 cm⁻¹; Figure S3: ¹H NMR spectrum of the ligand **1**; Figure S4: ¹H NMR spectrum of complex **2**; Figure S5: ¹³C NMR spectrum of ligand **1**; Figure S6: ¹³C NMR spectrum of complex **2**; Figure S7: Theoretical IR spectra of the *cis*- and *trans*-isomers of the complex **2**.

Author Contributions: Conceptualization, E.C., A.Š. and A.B.; methodology, A.B., M.A., Ž.Š., K.T., R.B., E.C. and A.Š.; software, E.C. and M.A.; formal analysis, Ž.Š., K.T., R.B., A.Š. and A.B.; investigation, E.C., M.A., A.Š. and A.B.; writing—original draft preparation, E.C., A.Š., M.A. and A.B.; writing—review and editing, M.A., Ž.Š., K.T., R.B., E.C., A.Š. and A.B.; visualization, E.C., M.A. and A.Š.; supervision, E.C., A.Š. and A.B. All authors have read and agreed to the published version of the manuscript.

Funding: This research was funded by the Ministry of Education Science and Technological Development of the Republic of Serbia grant number 451-03-68/2022-14/200113 and Faculty of Medicine of the University of Niš Internal project No. 40.

Institutional Review Board Statement: Not applicable.

Informed Consent Statement: Not applicable.

Data Availability Statement: Not applicable.

Acknowledgments: The financial support of this work by the project of the Ministry of Education, Science and Technological Development of the Republic of Serbia (number 451-03-68/2022-14/200113) and Internal project No. 40 of the Faculty of Medicine of the University of Niš is gratefully acknowledged.

Conflicts of Interest: The authors declare no conflict of interest. The funders had no role in the design of the study, in the collection, analyses, or interpretation of data, in the writing of the manuscript, or in the decision to publish the results.

Sample Availability: A sample of complex 2 is available from the authors.

References

1. Mohammed, H.S.; Tripathi, V.D. Medicinal applications of coordination complexes. *J. Phys. Conf. Ser.* **2020**, *1664*, 012070. [[CrossRef](#)]
2. Hossain, S.; Zakaria, C.M.; Kudrat-E-Zahan, M. Metal complexes as potential antimicrobial agent: A Review. *Am. J. Heterocycl. Chem.* **2018**, *4*, 1. [[CrossRef](#)]
3. Abdel-Rahman, L.H.; Abu-Dief, A.M.; El-Khatib, R.M.; Abdel-Fatah, S.M.; Seleem, A.A. New Cd(II), Mn(II) and Ag(I) Schiff base complexes: Synthesis, characterization, DNA binding and antimicrobial activity. *Int. J. Nanomater. Chem.* **2016**, *2*, 83–91. [[CrossRef](#)]
4. Jia, P.; Ouyang, R.; Cao, P.; Tong, X.; Zhou, X.; Lei, T.; Zhao, Y.; Guo, N.; Chang, H.; Miao, Y.; et al. Review: Recent advances and future development of metal complexes as anticancer agents. *J. Coord. Chem.* **2017**, *70*, 2175–2201. [[CrossRef](#)]
5. Ramadan, A.M.; Alshehri, A.A.; Bondock, S. Synthesis, physico-chemical studies and biological evaluation of new metal complexes with some pyrazolone derivatives. *J. Saudi Chem. Soc.* **2019**, *23*, 1192–1205. [[CrossRef](#)]
6. Wheate, N.J.; Walker, S.; Craig, G.E.; Oun, R. The status of platinum anticancer drugs in the clinic and in clinical trials. *Dalton Trans.* **2010**, *39*, 8113–8127. [[CrossRef](#)]
7. Hartmann, J.T.; Lipp, H.-P. Toxicity of platinum compounds. *Expert Opin. Pharmacother.* **2003**, *4*, 889–901. [[CrossRef](#)]
8. Kosmider, B.; Wyszynski, K.; Janik-Spiechowicz, E.; Osiecka, R.; Zyner, E.; Ochocki, J.; Ciesielska, E.; Wasowicz, W. Corrigendum to “Evaluation of the genotoxicity of cis-bis (3-aminoflavone) dichloroplatinum (II) in comparison with cis-DDP”. *Mutat. Res. Gen. Toxic. Environ. Mutag.* **2004**, *558*, 93–110. [[CrossRef](#)]
9. Jakupec, M.A.; Galanski, M.; Keppler, B.K. Tumour-inhibiting platinum complexes—State of the art and future perspectives. *Rev. Physiol. Biochem. Pharmacol.* **2003**, *146*, 1–53. [[CrossRef](#)]
10. Kalinowska-Lis, U.; Ochocki, J.; Matlawska-Wasowska, K. *Trans* geometry in platinum antitumor complexes. *Coord. Chem. Rev.* **2008**, *252*, 1328–1345. [[CrossRef](#)]
11. Rajic, Z.; Zorc, B.; Raic-Malic, S.; Ester, K.; Kralj, M.; Pavelic, K.; Balzarini, J.; De Clercq, E.; Mintas, M. Hydantoin derivatives of L- and D-amino acids: Synthesis and evaluation of their antiviral and antitumoral activity. *Molecules.* **2006**, *11*, 837–848. [[CrossRef](#)]
12. Kleemann, A.; Engel, J.; Kutscher, B.; Reichert, D. *Pharmaceutical Substances, Synthesis, Patents, Applications*, 4th ed.; Thieme: Stuttgart, Germany, 2001.
13. Puszyńska-Tuszkankow, M.; Daszkiewicz, M.; Maciejewska, G.; Adach, A.; Cieslak-Golonka, M. Interaction of hydantoins with transition metal ions: Synthesis, structural, spectroscopic, thermal and magnetic properties of $[M(H_2O)_4(phenytoinate)_2]$ $M = Ni(II), Co(II)$. *Struct. Chem.* **2009**, *21*, 315–321. [[CrossRef](#)]
14. Bakalova, A.; Buyukliev, R.; Momekov, G.; Ivanov, D.; Todorov, D.; Konstantinov, S.; Karaivanova, M. Synthesis, physicochemical and *in vitro* pharmacological investigation of new platinum (II) complexes with some cycloalkanespiro-5'-hydantoins. *Eur. J. Med. Chem.* **2005**, *40*, 590–596. [[CrossRef](#)]
15. Bakalova, A.; Buyukliev, R.; Tcholakova, I.; Momekov, G.; Konstantinov, S.; Karaivanova, M. Synthesis, physicochemical investigation and cytotoxic activity of new Pt(II) complexes with hydantoin ligands. *Eur. J. Med. Chem.* **2003**, *38*, 627–632. [[CrossRef](#)]
16. Battelli, M.G.; Polito, L.; Bortolotti, M.; Bolognesi, A. Xanthine oxidoreductase in cancer: More than a differentiation marker. *Cancer Med.* **2015**, *5*, 546–557. [[CrossRef](#)]
17. Šmelcerović, A.; Tomović, K.; Šmelcerović, Ž.; Petronijević, Ž.; Kocić, G.; Tomašić, T.; Jakopin, Ž.; Anderluh, M. Xanthine oxidase inhibitors beyond allopurinol and febuxostat; an overview and selection of potential leads based on *in silico* calculated physico-chemical properties, predicted pharmacokinetics and toxicity. *Eur. J. Med. Chem.* **2017**, *135*, 491–516. [[CrossRef](#)]
18. You, Z.-L.; Shi, D.-H.; Zhu, H.-L. The inhibition of xanthine oxidase by the Schiff base zinc(II) complex. *Inorg. Chem. Commun.* **2006**, *9*, 642–644. [[CrossRef](#)]
19. Li, Y.-G.; Shi, D.-H.; Zhu, H.-L.; Yan, H.; Ng, S.W. Transition metal complexes ($M=Cu, Ni$ and Mn) of Schiff-base ligands: Syntheses, crystal structures, and inhibitory bioactivities against urease and xanthine oxidase. *Inorg. Chim. Acta* **2007**, *360*, 2881–2889. [[CrossRef](#)]

20. You, Z.-L.; Shi, D.-H.; Xu, C.; Zhang, Q.; Zhu, H.-L. Schiff base transition metal complexes as novel inhibitors of xanthine oxidase. *Eur. J. Med. Chem.* **2008**, *43*, 862–871. [[CrossRef](#)]
21. Leigh, M.; Castillo, C.E.; Raines, D.J.; Duhme-Klair, A.K. Synthesis, activity testing and molybdenum(VI) complexation of Schiff bases Derived from 2,4,6-trihydroxybenzaldehyde investigated as xanthine oxidase inhibitors. *ChemMedChem* **2010**, *6*, 612–616. [[CrossRef](#)]
22. Ikram, M.; Rehman, S.; Khan, A.; Baker, R.J.; Hofer, T.S.; Subhan, F.; Qayum, M.; Faridooon; Schulzke, C. Synthesis, characterization, antioxidant and selective xanthine oxidase inhibitory studies of transition metal complexes of novel amino acid bearing Schiff base ligand. *Inorg. Chim. Acta* **2015**, *428*, 117–126. [[CrossRef](#)]
23. Özerkan, D.; Ertik, O.; Kaya, B.; Kuruca, S.E.; Yanardag, R.; Ülküseven, B. Novel palladium (II) complexes with tetradentate thiosemicarbazones. Synthesis, characterization, in vitro cytotoxicity and xanthine oxidase inhibition. *Investig. New Drugs* **2019**, *37*, 1187–1197. [[CrossRef](#)] [[PubMed](#)]
24. Cherneva, E.; Atanasova, M.; Buyukliev, R.; Tomovic, K.; Smelcerovic, Z.; Bakalova, A.; Smelcerovic, A. 3'-Methyl-4-thio-1 H-tetrahydropyranspiro-5'-hydantoin platinum complex as a novel potent anticancer agent and xanthine oxidase inhibitor. *Arch. Der Pharm.* **2020**, *353*, e2000039. [[CrossRef](#)] [[PubMed](#)]
25. Kushev, D.; Gorneva, G.; Taxirov, S.; Spassovska, N.; Grancharov, K. Synthesis, Cytotoxicity and antitumor activity of platinum(II) complexes of cyclopentanecarboxylic acid hydrazide. *Biol. Chem.* **1999**, *380*, 1287–1294. [[CrossRef](#)] [[PubMed](#)]
26. Nakamoto, K. *Infrared and Raman Spectra of Inorganic and Coordination Compounds*; Part III; Wiley: New York, NY, USA, 1978.
27. Nuttall, R. Characteristic metal-halogen vibrational frequencies of complexes with bivalent metal halides. *Talanta* **1968**, *15*, 157–169. [[CrossRef](#)]
28. Bednarski, P.J.; Ehrensperger, E.; Schoenenberger, H.; Burgemeister, T. Aqueous chemistry of mixed-amine *cis*- and *trans*platin analogues. Intramolecular preference for a kinetic six-membered ring over a thermodynamic five-membered ring ortho-platination product. *Inorg. Chem.* **1991**, *30*, 3015–3025. [[CrossRef](#)]
29. Pracharova, J.; Saltarella, T.; Muchova, T.R.; Scintilla, S.; Novohradsky, V.; Novakova, O.; Intini, F.P.; Pacifico, C.; Natile, G.; Ilik, P.; et al. Novel antitumor cisplatin and transplatin derivatives containing 1-methyl-7-azaindole: Synthesis, characterization, and cellular responses. *J. Med. Chem.* **2014**, *58*, 847–859. [[CrossRef](#)]
30. Cherneva, E.; Buyukliev, R.; Burdzhiev, N.; Michailova, R.; Bakalova, A. Synthesis, physico-chemical investigation, DFT calculations and cytotoxic activity of palladium complexes with 3'-amino-4-thio-1H-tetrahydropyranspiro-5'-hydantoin. *Bulg. Chem. Commun.* **2017**, *49*, 164–170.
31. Melník, M.; Mikuš, P. Structural aspects of monomeric platinum coordination complexes. *Mater. Sci. Appl.* **2014**, *5*, 512–547. [[CrossRef](#)]
32. Pereira, A.K.D.S.; Manzano, C.M.; Nakahata, D.H.; Clavijo, J.C.T.; Pereira, D.H.; Lustri, W.R.; Corbi, P.P. Synthesis, crystal structures, DFT studies, antibacterial assays and interaction assessments with biomolecules of new platinum(II) complexes with adamantane derivatives. *New J. Chem.* **2020**, *44*, 11546–11556. [[CrossRef](#)]
33. Bakalova, A.; Nikolova-Mladenova, B.; Buyukliev, R.; Cherneva, E.; Momekov, G.; Ivanov, D. Synthesis, DFT calculations and characterisation of new mixed Pt(II) complexes with 3-thiolanespiro-5'-hydantoin and 4-thio-1H-tetrahydropyranspiro-5'-hydantoin. *Chem. Pap.* **2016**, *70*, 93–100. [[CrossRef](#)]
34. Ahmad, S.; Nadeem, S.; Anwar, A.; Hameed, A.; Tirmizi, S.A.; Zierkiewicz, W.; Abbas, A.; Isab, A.A.; Alotaibi, M.A. Synthesis, characterization, DFT calculations and antibacterial activity of palladium(II) cyanide complexes with thioamides. *J. Mol. Struct.* **2017**, *1141*, 204–212. [[CrossRef](#)]
35. Subhajt Mukherjee, S.; Reddy, V.P.; Mitra, I.; Moi, S.C. *In vitro* kinetic based adduct formation mechanism of a cytotoxic Pt(II) complex with sulfur containing bio-relevant molecules and a theoretical approach. *Polyhedron* **2017**, *124*, 251–261. [[CrossRef](#)]
36. Frisch, M.J.; Trucks, G.W.; Schlegel, H.B.; Scuseria, G.E.; Robb, M.A.; Cheeseman, J.R.; Montgomery, J.A.; Vreven, T.; Kudin, K.N.; Burant, J.C.; et al. *Gaussian 03, Revision C.02*; Gaussian Inc.: Wallingford, CT, USA, 2004.
37. Stephens, P.J.; Devlin, F.J.; Chabalowski, C.F.; Frisch, M.J. *Ab Initio* calculation of vibrational absorption and circular dichroism spectra using Density Functional Force Fields. *J. Phys. Chem.* **1994**, *98*, 11623–11627. [[CrossRef](#)]
38. Lee, C.T.; Yang, W.T.; Parr, R.G. Development of the Colle-Salvetti correlation-energy formula into a functional of the electron density. *Physics* **1988**, *37*, 785–789.
39. Mosmann, T. Rapid colorimetric assay for cellular growth and survival: Application to proliferation and cytotoxicity assays. *J. Immunol. Methods* **1983**, *65*, 55–63. [[CrossRef](#)]
40. Konstantinov, S.M.; Eibl, H.; Berger, M.R. BCR-ABL influences the antileukaemic efficacy of alkylphosphocholines. *Br. J. Haematol.* **1999**, *107*, 365–374. [[CrossRef](#)]
41. Smelcerovic, Z.; Veljkovic, A.; Kocic, G.; Yancheva, D.; Petronijevic, Z.; Anderluh, M.; Smelcerovic, A. Xanthine oxidase inhibitory properties and anti-inflammatory activity of 2-amino-5-alkylidene-thiazol-4-ones. *Chem. Interact.* **2015**, *229*, 73–81. [[CrossRef](#)]
42. Cao, H.; Paufl, J.M. Hille, R. Substrate orientation and catalytic specificity in the action of xanthine oxidase: The sequential hydroxylation of hypoxanthine to uric acid. *J. Biol. Chem.* **2010**, *285*, 28044–28053. [[CrossRef](#)]
43. *Molecular Operating Environment (MOE)*, version MOE 2016.0801; Chemical Computing Group Inc.: Montreal, QC, Canada, 2016.